



Original Article

# Sensor Anchoring Improves the Correlation Between Intramuscular Pressure and Muscle Tension in a Rabbit Model

SHAWN M. O'CONNOR,<sup>1</sup> KENTON R. KAUFMAN,<sup>3</sup> SAMUEL R. WARD,<sup>2,4,5</sup>  
and RICHARD L. LIEBER<sup>2,4,6,7</sup>

<sup>1</sup>School of Exercise and Nutritional Sciences, San Diego State University, San Diego, CA, USA; <sup>2</sup>Department of Orthopaedic Surgery, University of California San Diego, La Jolla, CA, USA; <sup>3</sup>Department of Orthopedic Surgery, Mayo Clinic, Rochester, MN, USA; <sup>4</sup>Department of Bioengineering, University of California San Diego, La Jolla, CA, USA; <sup>5</sup>Department of Radiology, University of California San Diego, La Jolla, CA, USA; <sup>6</sup>Veteran's Administration San Diego Healthcare System, San Diego, CA, USA; and <sup>7</sup>Shirley Ryan AbilityLab and Northwestern University, 355 E. Erie Street, Chicago, IL 60611, USA

(Received 23 June 2020; accepted 18 September 2020; published online 1 October 2020)

Associate Editor Jane Grande-Allen oversaw the review of this article.

**Abstract**—Intramuscular pressure (IMP) shows promise for estimating individual muscle tension *in vivo*. However, previous pressure measurements show high variability during isometric contraction and poor correlation with tension during dynamic contraction. We hypothesized that enhanced sensor anchoring/orientation would improve tension estimation and thus developed a novel pressure sensor with a barbed housing. Sensors were inserted into the tibialis anterior (TA) of New Zealand White rabbits ( $N = 8$ ) both parallel and perpendicular to the fiber orientation. We measured muscle stress and IMP during both isometric and dynamic contractions. Passive stress showed good agreement for both insertion directions across muscle lengths (ICC > 0.8). Active stress and IMP agreement were good (ICC =  $0.87 \pm 0.04$ ) for perpendicular insertions but poor (ICC =  $0.21 \pm 0.22$ ) for parallel insertions across both dynamic contractions and isometric contractions within the muscle's range of motion. These findings support use of IMP measurements to estimate muscle tension across a range of contraction conditions.

**Keywords**—Isometric contraction, Dynamic contraction, Force–length relationship, Force–velocity relationship.

## ABBREVIATIONS

IMP Intramuscular pressure  
COV Coefficient of variation  
TA Tibialis anterior

ROM Range of motion  
HA Hyaluronic acid  
PCSA Physiological cross-sectional area  
COD Coefficient of determination  
ICC Intraclass correlation coefficient

## INTRODUCTION

Assessment of *in vivo* muscle function is a challenge that limits clinical evaluation of human muscle health. Direct measures of real-time muscle tension, as would be desired during clinical gait testing, are highly invasive and typically confined to animal studies. Ultrasound elastography provides a rough estimate of muscle tension but only during quasi steady-state conditions.<sup>13</sup> Intramuscular pressure (IMP), the fluid pressure within muscle, is an attractive proxy for real-time muscle tension as IMP and muscle stress are directly related based on muscle fiber curvature and fiber depth.<sup>14,24</sup> IMP during gait resembles the human ground reaction force profile<sup>2</sup> and isometric and isokinetic joint torque<sup>1,26</sup> using relatively invasive (16–18 g needle) catheter sensors in research settings. More recent fiber optic sensors are clinically attractive because of their small size (< 300  $\mu\text{m}$  diameter<sup>4</sup>) and insensitivity to hydrostatic artifacts during sensor movement.<sup>6,16</sup>

While seemingly ideal for clinical use, fiber optic IMP sensors have demonstrated limited capacity to predict *in vivo* muscle tension. For isometric contrac-

Address correspondence to Richard L. Lieber, Shirley Ryan AbilityLab and Northwestern University, 355 E. Erie Street, Chicago, IL 60611, USA. Electronic mail: rlieber@sralab.org

tions, IMP was previously correlated with both passive and active muscle tension.<sup>7,9,17</sup> However, IMP coefficients of variation (COV) often exceeded 60% during active contractions and even negative pressures were recorded during unloaded passive conditions.<sup>7</sup> Under dynamic conditions, IMP and muscle tension were well-correlated for shortening (concentric) contractions, but not for lengthening (eccentric) contractions or isotonic conditions.<sup>9,28</sup> These observed dynamic muscle stress-IMP dissociations were attributed to poor sensor anchoring which was confirmed using high-speed videography.<sup>28</sup>

We hypothesized that improved sensor anchoring would increase the muscle stress-IMP correlation. Previous fiber optic designs incorporated a single-barbed polyimide housing to protect the pressure transducer and secure the sensor within muscle tissue.<sup>8,28</sup> We believed that redesigning the housing using a stronger material and increasing barb number would improve the stability of sensor anchoring. Indeed, recent use of a four-barbed nitinol housing demonstrated increased anchoring forces over previous designs and improved muscle force-pressure correlation during isometric contractions at optimal muscle length.<sup>10</sup>

We also hypothesized that the sensor insertion orientation would influence muscle stress-IMP correlation. IMP sensors have traditionally been inserted parallel to the muscle fiber shortening direction to allow sliding relative to adjacent fibers and to minimize muscle trauma.<sup>25</sup> However, relative sensor-fiber motion may cause motion artifacts in transducer tipped sensors due to measuring of pistoning forces along the interstitial column.<sup>5,21</sup> Relative movement of the transducer relative to the muscle fibers has, in fact, already been demonstrated.<sup>28</sup> Perpendicular sensor insertion may avoid this artifact and improve sensitivity to transverse forces associated with muscle pressure by aligning the sensing surface with the lateral muscle axis. Perpendicular insertions may also facilitate anchoring by allowing housing barbs to engage with muscle fibers. We predicted that perpendicular insertions would improve muscle stress-IMP agreement compared to parallel insertions. The purpose of this study was, therefore, to evaluate whether IMP is a valid surrogate for muscle stress using a new nitinol housing-based pressure microsensor and determine preferred sensor insertion orientation.

## MATERIALS AND METHODS

### *Pressure Sensor*

Pressure sensors were composed of a fiber optic microsensor paired with a barbed nitinol housing, which isolated the pressure transducer from the tissue

environment and improved anchoring.<sup>10</sup> The 260  $\mu\text{m}$  diameter microsensor (model FOP-M260, FISO Technologies, Inc., Quebec, Canada) is rated by the manufacturer at 2 mmHg accuracy and  $< 0.1$  mmHg resolution. The housing was formed from 457  $\mu\text{m}$  outer diameter nitinol tubing laser cut to form four proximally oriented barbs (Fig. 1a). The barb shape was designed to improve sensor anchoring during IMP measurements while allowing safe removal of the sensor following testing. The housing was then glued to the sensor cable, with the pressure-transducing surface recessed from the housing end Fig. 1b. Also see Fig. 1 of Reference 10.

### *Active Mechanics Surgery*

Tibialis anterior (TA) muscles of eight New Zealand White rabbits (mass =  $3.59 \pm 0.04$  kg, mean  $\pm$  SEM) were chosen for force and pressure measurements based on accessibility and parallel fiber arrangement.<sup>19</sup> All procedures were approved by and conducted in accordance with the University of California Institutional Animal Care and Use Committee.

Animal preparation and measurement of dynamic contractile properties were performed as described previously.<sup>7,28</sup> Briefly, rabbits were anesthetized subcutaneously with a ketamine-xylazine cocktail (35 and 5 mg/kg, respectively) and maintained on 2% isoflurane at 2 L/min through a facemask. Heart rate and oxygen saturation were monitored and a hot water pad maintained body temperature. A midline incision was made from ankle to mid-thigh and fascia was removed to aid visualization of probe insertion and sensor anchoring. Muscle length was measured with the ankle joint at full plantarflexion and full dorsiflexion to define the muscle's physiological range of motion (ROM). The hind limb was immobilized in a custom jig *via* compression pins at the femoral condyles and malleoli (Fig. 1c). The biceps femoris insertion was split and a cuff electrode was placed around the peroneal nerve for direct stimulation (S48 Stimulator; Grass Technologies, Warwick, RI). The TA tendon was then transected and clamped to a servomotor at the muscle-tendon junction (Cambridge Model 300B; Aurora Scientific, Aurora, ON) and aligned with the force-generating axis of the motor. Muscle and tendon were regularly irrigated with phosphate-buffered saline.

Sensors were inserted *via* 22-gauge angiocatheters that were first inserted at mid-belly and depth of approximately 2 mm. We placed  $\sim 25$   $\mu\text{L}$  of hyaluronic acid (HA) near the catheter tip, to provide a stable aqueous environment. Catheters were then withdrawn and housing barbs were anchored by pulling on the fiber optic cable while applying local pressure to the muscle. Three sensors were inserted in each

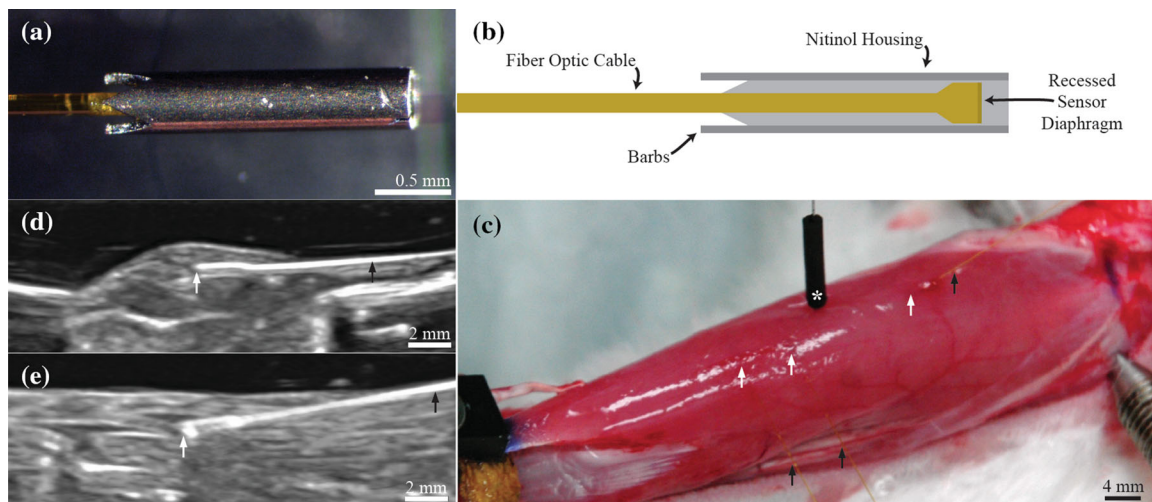


**FIGURE 1.** Experimental apparatus used to measure force–IMP relationship. (a) Pressure sensor with nitinol housing and four proximally facing barbs. (b) Longitudinal cross-section drawing of sensor and housing. (c) Rabbit hindlimb immobilized in custom jig *via* tightened screws at the lateral femoral condyle and malleoli. White asterisks indicates electromyography sensor. White arrows denote approximate location of sensor tips within the muscle. Black arrows indicate sensor fiber optic cables exiting the muscle. (d) Transverse plane B-mode ultrasound image of perpendicular orientation sensor within muscle compartment. (e) Sagittal plane ultrasound image depicting parallel orientation sensor.

muscle, two oriented perpendicular to the muscle fibers and one parallel. This arrangement allowed all sensors to be located at the muscle mid-line within the muscle belly and with sufficient spacing between them. Ultrasound images (t3200, Terason, Burlington, MA) confirmed mid-belly placement and measured sensor depth (Figs. 1d and 1e). Individual sensors were reinserted if robust IMP signals were not recorded upon initial muscle stimulation. At most, five insertions were allowed per muscle to minimize trauma, and reinsertions were prioritized to ensure at least one perpendicular and one parallel insertion functioned per muscle. IMP signals from duplicate perpendicular insertions were time averaged. In total, 14 perpendicular insertions and 8 parallel insertions from 8 different animal subjects were tested.

#### *Trial Protocol*

Each trial consisted of 100 Hz tetanic contractions (pulse width: 0.3 ms) over a 500 ms train. All contractions were performed at supramaximal voltage, determined as 150% of the stimulation voltage eliciting maximum twitch force. Length, force, and IMP were recorded using acquisition hardware (USB-6356; National Instruments, Austin, TX) and a custom-written LabView program (National Instruments) sampling at 8 kHz. Three-minute rest intervals were interposed between all contractions to reduce fatigue.

Muscle length changes during isometric, concentric, or eccentric contractions were referenced relative to optimal muscle length ( $L_{m0}$ ).  $L_{m0}$  was identified by

locating peak force production using repeated-pulse contractions<sup>22</sup> to reduce fatigue. Optimal fiber length ( $L_{f0}$ ) was calculated based on known fiber-to-muscle length ratio of 0.67.<sup>19</sup> Two isometric contractions at  $L_{m0}$  were tested both before and after probe insertion to measure the insertion effect on force production. The isometric length-tension measurements then began at  $L_{m0}$  and ranged from  $-35$  to  $35\%$   $L_{f0}$  in increments of  $5\%$   $L_{f0}$ .

For concentric contractions, muscle length was initially set to  $L_{m0} + 5\%L_{f0}$ . After muscle activation, length was held constant for 200 ms and isometric force generated (Figs. 2b and 2c). Then, length was decreased by  $10\%$   $L_f$  at a selected velocity and muscle length was again held constant, permitting redevelopment of isometric tension at the shorter length. Concentric velocity was increased in  $1.0 L_f/s$  increments ranging from  $0.5$  to  $4.5 L_f/s$ . For eccentric contractions, length was first set to  $L_{m0} - 5\%L_{f0}$ . The protocol for the concentric contractions was replicated using positive length ramps of  $1$  and  $2 L_f/s$  (Fig. 2d).

Upon completion of contractile testing, animals were euthanized with pentobarbital (120 mg/kg) and muscles were removed, blotted dry and then weight and pennation angle measured.

#### *Analysis and Statistics*

Individual muscle force and IMP traces were filtered using a first-order low-pass Butterworth filter (100 Hz cut-off). Passive values were measured by averaging over the 100 ms period prior to muscle stimulation.

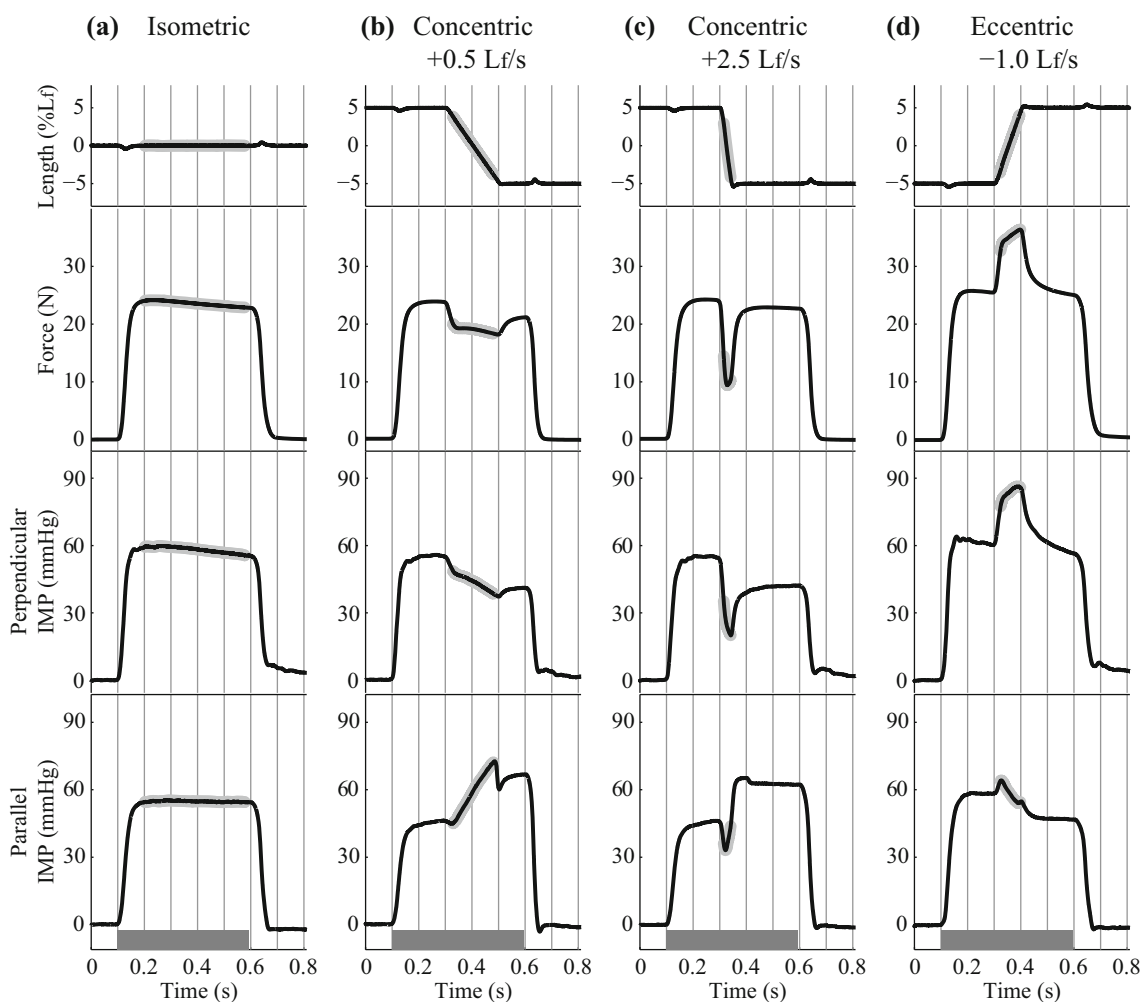


**FIGURE 2.** Sample filtered traces of muscle length deviations from optimal length ( $\%L_t$ ), active muscle force (N), and IMP (mmHg) under parallel and perpendicular insertion orientations at range of muscle velocities. Solid dark gray bars indicate muscle activation intervals. Perpendicular orientation IMP signals correspond with velocity-dependent changes in muscle force. Average force and IMP values during periods of constant velocity (light gray) were used to construct length and velocity dependent relationships with force and IMP. Linear regression calculated the correlation between force and IMP traces during the displayed time interval.

Active force and IMP traces were calculated by subtracting the passive values from respective total traces. Force was then converted to muscle stress by dividing by the muscle's physiological cross-sectional area (PCSA),<sup>23</sup> where  $PCSA = (m \cdot \cos(\Theta)) / (L_{f0} \cdot \rho)$  and  $m$  is the muscle mass,  $\Theta$  is the pennation angle, and  $\rho$  is the muscle density value of  $1.0597 \text{ g/cm}^3$ . To characterize the correlation between the active stress and IMP traces, coefficient of determination (COD) was quantified using linear regression. Active stress and active IMP values were determined by averaging over the period during contraction of constant velocity (Fig. 2).

Values from each trial were analyzed as follows: Distribution normality was determined using the Anderson–Darling test and statistical tests were selected accordingly. Isometric muscle stress recorded

before and after IMP probe insertion were compared using a Wilcoxon sign rank test. Peak stress ( $P_0$ ) and peak IMP ( $I_0$ ) for both insertion directions were then calculated from isometric contractions at  $L_{m0}$  following insertion.  $I_0$  between the two insertion directions were compared using a paired  $t$  test. CODs were compared with a Scheirer–Ray–Hare test for the length-dependent (main effects: muscle length and insertion direction) and velocity-dependent (main effects: muscle velocity and insertion direction) trial series. IMP values for each trial were then converted to predicted stress by multiplying each measure by the calibration factor ( $P_0/I_0$ ). Intraclass correlation coefficients (ICC) quantified the absolute agreement between predicted and measured stress values, where an ICC between 0.5 and 0.75, between 0.75 and 0.9, and greater than 0.9 were defined as moderate, good,



and excellent agreement, respectively.<sup>18</sup> For the length-dependent trials, ICC values were calculated for the ascending limb (lengths  $< L_{m0}$ ), the descending limb (lengths  $> L_{m0}$ ), and all isometric contractions as previously described.<sup>14</sup> Differences in limb region and insertion direction were compared with a Scheirer–Ray–Hare two-factor test. For the velocity-dependent trials, ICC values were calculated for the concentric, eccentric, and all dynamic contractions. Differences in velocity direction and insertion direction were compared with a two-way repeated-measures ANOVA.

All analyses and statistical computations were performed in Matlab with a Type I error rate ( $\alpha$ ) of 0.05. Values are presented as mean  $\pm$  SEM (standard error of the mean) unless otherwise stated.

## RESULTS

### *Stress and IMP Traces*

For isometric contractions, both insertion directions produced square-wave IMP traces in response to isometric force production (Fig. 2). However, for dynamic contractions, only perpendicular insertion produced velocity-dependent IMP traces that mimicked force traces, with force and IMP decreasing and increasing during the concentric and eccentric contraction intervals, respectively. In contrast, parallel insertion produced velocity-dependent IMP changes that were less correlated with and, in some cases, opposite to force changes, as reported previously.<sup>28</sup> In all cases, IMP measures demonstrated a comparatively slower decline to baseline after cessation of stimulation compared to the corresponding force record.

Correlation between isometric muscle stress and IMP traces at  $L_{m0}$  demonstrated that IMP explained  $86 \pm 8\%$  of the variance in contractile stress (i.e.,  $r^2 = 0.86$ ). Correlation further varied as a function of muscle length and velocity. Across isometric conditions, this value for coefficient of determination (COD) varied significantly with muscle length ( $p < 0.01$ ) and were higher for the parallel insertions ( $p < 0.001$ ) (Table 1). Categorizing lengths as either shorter than, within, or longer than the muscle's ROM ( $-11.5$  to  $16.2\% L_{m0}$ ), revealed a significant main effect of length region ( $p < 0.001$ ), with significantly lower COD at lengths shorter than the ROM compared to both longer length regions (both  $p < 0.001$ ). Across dynamic conditions tested, COD varied significantly with muscle velocity ( $p < 0.001$ ) but not insertion direction ( $p = 0.43$ ), with eccentric contraction values significantly higher than concentric values ( $p < 0.001$ ) (Table 2).

### *Baseline Comparisons*

Peak active stress ( $P_0$ ) was  $246.8 \pm 9.8$  kPa, which compares well with literature values for fast mammalian muscle.<sup>3</sup> Insertion of three sensors resulted in a small but significant 5.0% reduction in mean peak stress ( $p < 0.05$ ). Peak active IMP ( $I_0$ ) for the perpendicular and parallel insertions ( $64.6 \pm 7.0$  mmHg and  $37.1 \pm 5.8$  mmHg, respectively) were significantly different from each other ( $p < 0.05$ ), with parallel values similar to previous reports.<sup>7,28</sup> These baseline measures yield COVs of 11.2, 30.6, and 44.4% for active stress, perpendicular IMP, and parallel IMP, respectively. Measured sensors depths for the perpendicular and parallel insertions were not significantly different ( $p = 0.20$ ) with values of  $0.17 \pm 0.01$  and  $0.21 \pm 0.02$  cm, respectively. While IMP increases linearly with depth,<sup>20</sup> normalizing IMP values to a constant depth did not vary the statistics between insertion directions or improve precision.

The ratio between  $P_0$  and  $I_0$  was computed after insertion and before beginning the velocity-dependent trial series, with values of  $4.22 \pm 0.56$  and  $7.97 \pm 1.29$  kPa/mmHg for perpendicular and parallel insertions, respectively. Ratios were recomputed before the length-dependent trial series, with respective values of  $4.97 \pm 1.14$  and  $8.54 \pm 1.93$  kPa/mmHg. Ratios did not significantly vary between first and second calculations ( $p = 0.42$ ).

### *Length Dependence*

As expected, the active stress-length curve was described by ascending and descending limbs centered about  $L_{m0}$  (Fig. 3a). The active IMP-length relationship for perpendicular insertions was similarly characterized (Fig. 3b). However, IMP proved comparatively more variable and dropped faster than expected at longer lengths. IMP values did not follow expected trends for parallel insertions with large increases relative to  $I_0$  at shorter lengths.

Significant agreement was observed between active stress and IMP as a function of muscle fiber length for perpendicular but not parallel insertion (Table 3). Average ICC for perpendicular insertion was  $0.69 \pm 0.06$  (median = 0.74). In contrast, the average ICC for parallel insertion was  $-0.01 \pm 0.07$  (median =  $-0.05$ ), with no individual values reaching significance ( $p = 0.053$ – $0.85$ ). Agreement for perpendicular insertion was significantly higher than parallel insertions across ascending and descending limbs ( $p < 0.001$ ). Agreement for the ascending and descending limbs was not significantly different across insertion directions ( $p = 0.055$ ) (Table 3).

**TABLE 1. Average coefficients of determination between active muscle stress and IMP signals at each muscle length.**

Muscle length (% $L_t$ )	Perpendicular			Parallel		
	Mean (SEM)	Min	Max	Mean (SEM)	Min	Max
- 35	0.49 (0.09)	0.24	0.87	0.25 (0.19)	- 0.53	0.80
- 30	0.49 (0.13)	- 0.27	0.93	0.50 (0.18)	- 0.30	0.93
- 25	0.28 (0.22)	- 0.80	0.97	0.77 (0.07)	0.46	0.98
- 20	0.45 (0.18)	- 0.52	0.98	0.81 (0.09)	0.23	0.97
- 15	0.64 (0.13)	0.05	0.98	0.90 (0.04)	0.61	0.99
- 10	0.80 (0.06)	0.50	0.99	0.85 (0.08)	0.41	1.00
- 5	0.79 (0.07)	0.36	0.99	0.82 (0.09)	0.36	1.00
0	0.80 (0.04)	0.28	0.98	0.73 (0.15)	- 0.26	1.00
5	0.76 (0.09)	0.37	0.96	0.79 (0.11)	0.12	0.99
10	0.73 (0.10)	0.25	0.97	0.86 (0.08)	0.36	1.00
15	0.67 (0.11)	0.00	0.95	0.90 (0.06)	0.49	1.00
20	0.68 (0.18)	- 0.53	0.94	0.91 (0.04)	0.71	0.99
25	0.80 (0.08)	0.31	0.95	0.95 (0.01)	0.91	0.99
30	0.64 (0.16)	- 0.12	0.96	0.96 (0.01)	0.94	1.00
35	0.39 (0.23)	- 0.50	0.96	0.92 (0.02)	0.79	0.99

**TABLE 2. Average coefficients of determination between active muscle stress and IMP signals at each muscle velocity, where lengthening and shortening are indicated by negative and positive velocities, respectively.**

Muscle velocity ( $L_t/s$ )	Perpendicular			Parallel		
	Mean (SEM)	Min	Max	Mean (SEM)	Min	Max
- 2.0	0.75 (0.08)	0.30	0.96	0.73 (0.12)	0.14	1.00
- 1.0	0.81 (0.07)	0.38	0.98	0.69 (0.14)	- 0.02	0.99
0.0	0.93 (0.02)	0.81	0.99	0.89 (0.06)	0.54	1.00
0.5	0.79 (0.05)	0.57	0.95	0.56 (0.13)	- 0.10	0.94
1.5	0.63 (0.12)	0.05	0.93	0.53 (0.12)	- 0.08	0.94
2.5	0.59 (0.13)	- 0.07	0.91	0.53 (0.13)	- 0.13	0.95
3.5	0.59 (0.13)	- 0.06	0.89	0.55 (0.13)	- 0.03	0.96
4.5	0.56 (0.14)	- 0.18	0.89	0.47 (0.18)	- 0.49	0.96

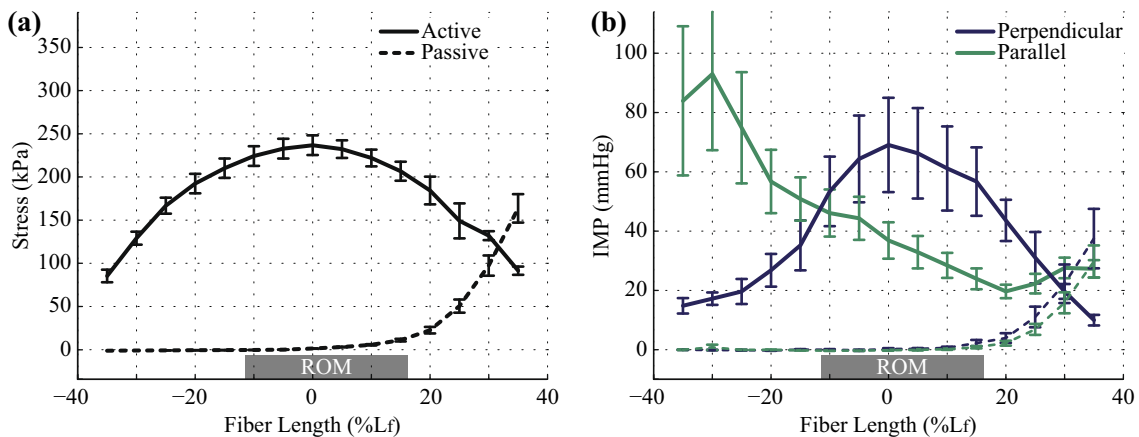


**FIGURE 3. (a) Average relationship between muscle stress (kPa) and fiber length change (% $L_t$ ). Active and passive stress are denoted by solid and dashed lines, respectively. Solid dark gray bars indicate average muscle range of motion. (b) Average relationship between IMP (mmHg) and fiber length change (% $L_t$ ) measured from pressure sensors inserted perpendicular (blue) and parallel (green) to muscle fibers. Each data point is presented as mean  $\pm$  SEM for eight animals.**

**TABLE 3. Average agreement between normalized stress and normalized IMP values across muscle length conditions.**

Insertion Direction	Contraction Type	ICC			
		Mean (SEM)	Median (IQR)	Min	Max
Perpendicular	Active	0.69 (0.06)	0.74 (0.19)	0.35	0.88
	Ascend	0.56 (0.19)	0.69 (0.31)	− 0.68	0.99
	Descend	0.88 (0.04)	0.89 (0.11)	0.67	0.99
	Passive	0.85 (0.05)	0.86 (0.21)	0.62	0.99
Parallel	Active	− 0.01 (0.07)	− 0.05 (0.16)	− 0.28	0.42
	Ascend	− 0.11 (0.11)	− 0.17 (0.21)	− 0.39	0.64
	Descend	0.28 (0.12)	0.21 (0.36)	− 0.35	0.82
	Passive	0.84 (0.09)	0.93 (0.20)	0.25	0.99

Passive IMP mimicked the exponential shape of the passive stress–length curve (Fig. 3) at lengths above  $L_{m0}$  and maintained near zero values for lengths below  $L_{m0}$ . Average ICC value was  $0.85 \pm 0.05$  and  $0.84 \pm 0.09$  for perpendicular and parallel insertion, respectively, and there was no significant difference between orientations ( $p = 0.94$ ).

#### Velocity Dependence

The active stress–velocity curve matched the expected rectangular hyperbola shape (Fig. 4a). During eccentric contractions (negative velocities), muscle stress was approximately 50% higher than  $P_0$ , as previously reported.<sup>11</sup> For concentric contractions, muscle stress monotonically decreased with increasing concentric velocity.<sup>12,15</sup>

The shape of the IMP–velocity curve for perpendicular insertions followed the stress–velocity relationship but with much higher variability (Fig. 4b). During eccentric contractions, IMP increased to a value 100% higher than  $I_0$  and for concentric contractions, IMP decreased monotonically relative to  $I_0$ . In contrast, the IMP–velocity curve for parallel insertions varied comparatively little with concentric velocity.

Significant agreement was found between active stress and IMP as a function of velocity for perpendicular but not parallel insertions (Table 4). Average ICC value was  $0.89 \pm 0.04$  (all  $p < 0.05$ , median = 0.92) for perpendicular insertions and  $0.19 \pm 0.25$  (median = 0.17) for parallel insertions, with no individual parallel values reaching significance ( $p = 0.053$ – $0.85$ ). Agreement was significantly higher for perpendicular insertions compared to parallel insertions across contraction velocities ( $p < 0.05$ ), and agreement for eccentric contractions was significantly higher than for concentric contractions across insertion directions ( $p < 0.001$ ) (Table 4).

Agreement was also quantified across conditions most likely to occur during natural movements (iso-

metric contractions within the ROM and all dynamic contractions). Across these conditions, significant agreement was observed between active stress and IMP for perpendicular (ICC =  $0.87 \pm 0.04$ ) but not parallel insertions (ICC =  $0.21 \pm 0.22$ ).

## DISCUSSION

These data demonstrate that IMP can serve as a proxy for both active and passive relative muscle tension within a range of the tested contraction conditions when the transducer is appropriately anchored and placed perpendicular to the fiber direction. This nitinol housing-based pressure sensor improved the average stress–IMP agreement and IMP COV compared to our previous experiments that tested polyamide housing-based sensors inserted parallel to the fibers. The excellent agreement (ICC = 0.89) between IMP and stress across eccentric and concentric contractions contrasts with previous poor agreement resulting from declines in IMP during eccentric contractions and relatively large COV during concentric contractions. See Fig. 2 in Reference 28.

While IMP measured from polyamide housed sensors inserted parallel to the fibers has previously shown some agreement with muscle stress for isometric conditions, we measured higher agreement for both active tension (ICC of 0.69 vs. 0.48) and passive tension (ICC of 0.85 vs. 0.80) across similar muscle lengths.<sup>29</sup> Related to this improved agreement, we demonstrated improved COV for the isometric conditions (COV at  $L_{m0}$  of 30% vs. 86%).<sup>7</sup> We also measured a stable near-zero IMP during unloaded passive conditions (Fig. 3), whereas significant paradoxically-negative pressures were previously reported.<sup>7,29</sup> Although the isometric agreement only improved to a moderate level (ICC = 0.69), when considering the full range of fiber lengths, agreement increased considerably (ICC of 0.87) when compiling conditions most likely to oc-

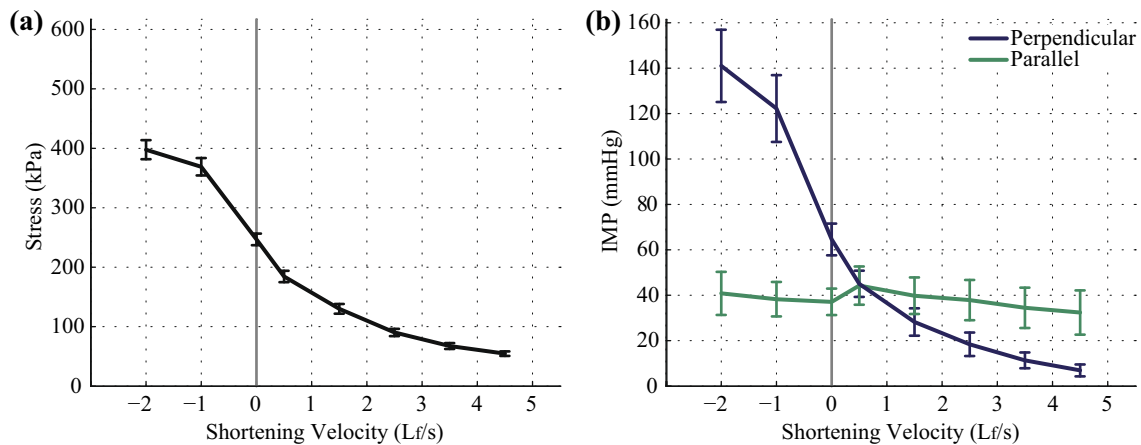


**FIGURE 4.** (a) Average relationship between muscle stress (kPa) and muscle velocity ( $L_t/s$ ), where lengthening and shortening are indicated by negative and positive velocities, respectively. (b) Average relationship between IMP (mmHg) and velocity ( $L_t/s$ ) measured from pressure sensors inserted perpendicular (blue) and parallel (green) to muscle fibers. Each data point is presented as mean  $\pm$  SEM for eight animals.

**TABLE 4.** Average agreement between normalized stress and normalized IMP values across muscle velocity conditions.

Insertion Direction	Contraction Type	ICC			
		Mean (SEM)	Median (IQR)	Min	Max
Perpendicular	Eccentric + Concentric	0.89 (0.04)	0.92 (0.14)	0.64	0.99
	Concentric	0.78 (0.07)	0.83 (0.26)	0.41	0.99
	Eccentric	0.97 (0.01)	0.98 (0.05)	0.91	1.00
Parallel	Eccentric + Concentric	0.19 (0.25)	0.17 (1.22)	- 0.85	0.99
	Concentric	0.07 (0.25)	- 0.06 (1.15)	- 0.95	0.99
	Eccentric	0.33 (0.23)	0.39 (1.04)	- 0.73	0.97

cur during natural movements (isometric contractions within the ROM and dynamic contractions near  $L_{m0}$ ). This finding suggests that the IMP measures using this transducer approach are valid as a proxy for active tension within the ROM.

In contrast, IMP was not a valid proxy for active tension for parallel insertions over the range of contraction conditions tested. Isometric contractions with parallel insertions did produce higher COD between muscle stress and IMP, as was found previously with the same sensor for isometric contractions at neutral muscle length.<sup>10</sup> However, these values agreed poorly with muscle stress as a function of muscle length and velocity. These findings suggest that the parallel insertions adequately captured the nature of force development and relaxation under isometric conditions but did not capture amplitude variations of force associated with changing muscle length and velocity. Under dynamic conditions, IMP demonstrated previously observed drops during eccentric contractions.<sup>28</sup> Unlike our previous isometric measurements,<sup>7,29</sup> we found no agreement for isometric contractions (mean ICC = - 0.01) due to unexpected high values mea-

sured on the ascending limb. However, parallel insertions did produce good agreement for passive stress, suggesting that the sensors were functioning and transducing IMP.

Our findings clearly indicate that anchored, perpendicular sensor insertion improved muscle stress estimation. We hypothesized that perpendicular insertions would improve muscle stress-IMP agreement by both enhancing anchoring effectiveness and minimizing motion-related pistoning artifacts. While perpendicular insertions produced superior muscle stress-IMP agreement compared to parallel insertions, we cannot distinguish whether improved anchoring, reduced pistoning artifacts, or both led to this improvement. However, a parallel inserted catheter sensor with a circumferential transducing surface (i.e. transducing surface perpendicular to fibers) previously demonstrated minimal motion artifacts, suggesting that reduced pistoning and better alignment of the sensor with transverse muscle forces may have had a significant effect.<sup>21</sup> Also, our anecdotal experience suggests that the housing barbs more readily attached for perpendicular insertions.



Our findings also demonstrate that the four-barbed nitinol housing-based sensor design did not sufficiently improve muscle stress estimation compared to a previous single-barbed polyamide housing based sensor for parallel insertions. We hypothesized that the new nitinol housing design would improve muscle stress-IMP correlations by increasing the anchoring surface area and improving barb integrity. Although we did not compare the two designs in this study, the nitinol design has demonstrated improved anchoring based on pullout tests.<sup>10</sup> We did attempt to measure relative probe-fiber movement by performing a second eccentric trial at 1  $L_f/s$  while capturing ultrasound video of parallel sensors. However, the ultrasound contrast was too poor to accurately measure sensor movements with respect to the fibers and therefore justify dynamic anchoring. Regardless, improved anchoring for parallel insertions did not appear to sufficiently improve agreement between muscle stress and IMP.

Our findings provide support and instruction for future use of the fiber optic IMP sensor to estimate individual muscle stresses in human subjects. Although, previous IMP experiments used parallel insertions to minimize muscle trauma associated with relatively large (16–18 g) catheter sensors, the smaller fiber optic sensors (inserted with 22 g catheters) mitigate concern for muscle trauma and patient discomfort. All IMP recordings should incorporate a validation procedure, as we found that individual sensors would occasionally require an immediate second insertion to produce a robust IMP signal or that sensors would lose signal strength after many trials. Therefore, after probe insertions, subjects should complete a step-like maximum voluntary contraction or a repeatable non-maximum contraction (*e.g.*, sudden toe lifts against body weight). Sensors should be immediately reinserted if the IMP signal does not display a step-like shape or the expected muscle-dependent magnitude. This validation trial should then be repeated at the end of or periodically throughout the experiment to track changes in signal quality. Use of two probes per muscle will increase the likelihood of retaining at least one sensor with stable signal quality.

This study is subject to several limitations. First, we tested IMP in TA muscles where the fascia and skin were cleared from the muscle surface. Movement of these tissues relative to the muscle belly during contractions may transmit forces along the sensor fiber optic cable to the sensor housing and increase sensor motion artifacts. However, an intact anterior compartment previously provided little improvement to the isometric stress-IMP relationship as a function of muscle length<sup>29</sup> so this limitation may be in theory only. Second, we visually observed varying levels of

tissue accumulation within the housing recess area in a majority of the sensors following testing. Tissue occlusion may induce IMP variability by either blocking pressure transmission to the transducing surface<sup>27</sup> or mechanically impinging on the transducer. Previous use of this sensor correlated tissue occlusion with increased IMP values, supporting a mechanical interference explanation.<sup>10</sup> In this experiment, it was difficult to associate sensor performance with tissue accumulation given the large number of trials performed and the uncertainty of tissue accumulation timing. Third, pilot experimentation revealed that injection of HA into the insertion site prior to insertion improved the muscle stress-IMP correlations during individual trials over injection of saline or no injection (data not shown). While HA injections are routinely used to treat joint pain, non-therapeutic injections may not be desirable for human subjects. We hypothesize that HA stabilizes the fluid environment around the sensor tip and provides more consistent transduction from the muscle to the recessed transducing surface. Previous infusion-based IMP sensors (wick, catheter pump) intrinsically maintained this fluid environment by providing a steady saline flow into the tissue.<sup>1,26</sup>

Finally, we were unable to predict muscle stress from IMP *a priori*. Although the theoretical relationship between muscle stress and IMP based on sensor depth and fiber curvature<sup>24</sup> may allow direct conversion of IMP into muscle stress, this conversion would only be possible when sensor depth and fiber curvature are readily measured with ultrasound or another imaging technique. In this study, ultrasound contrast was not sufficient to reliably determine fiber curvature. In this case, normalizing all IMP values by  $I_0$  will yield a linear approximation of muscle stress where 100% is considered isometric maximum voluntary contraction. This method is analogous to EMG protocols that normalize EMG signals based on the measurement during isometric maximum voluntary contraction.

## ACKNOWLEDGMENTS

We are grateful to Shannon Bremner and Mary Esparza for their technical assistance and Dr. Koichi Masuda for valuable experimental advice. We thank Elisabeth Jensen, Shanette Go, Loribeth Evertz, and FISO Corporation for their contribution to the design, development, and manufacturing of the pressure microsensor. This study was supported by National Institute of Health Grants P30AR061303, R24HD050837, R01HD031476, and the Department of Veterans Affairs grant numbers I01RX002462 and IK6 RX003351.

## CONFLICT OF INTEREST

The authors declare that they have no conflicts of interest.

## REFERENCES

- <sup>1</sup>Aratow, M., R. E. Ballard, A. G. Crenshaw, J. Styf, D. E. Watenpugh, N. J. Kahan, and A. R. Hargens. Intramuscular pressure and electromyography as indexes of force during isokinetic exercise. *J. Appl. Physiol.* 74(2634–2640):1993, 1985.
- <sup>2</sup>Ballard, R. E., D. E. Watenpugh, G. A. Breit, G. Murthy, D. C. Holley, and A. R. Hargens. Leg intramuscular pressures during locomotion in humans. *J. Appl. Physiol.* 84(1976–1981):1998, 1985.
- <sup>3</sup>Close, R. I. Dynamic properties of mammalian skeletal muscles. *Physiol. Rev.* 52:129–197, 1972.
- <sup>4</sup>Cottler, P. S., W. R. Karpen, D. A. Morrow, and K. R. Kaufman. Performance characteristics of a new generation pressure microsensor for physiologic applications. *Ann. Biomed. Eng.* 37:1638–1645, 2009.
- <sup>5</sup>Crenshaw, A. G., J. R. Styf, and A. R. Hargens. Intramuscular pressures during exercise: an evaluation of a fiber optic transducer-tipped catheter system. *Eur. J. Appl. Physiol. Occup. Physiol.* 65:178–182, 1992.
- <sup>6</sup>Crenshaw, A. G., J. R. Styf, S. J. Mubarak, and A. R. Hargens. A new “transducer-tipped” fiber optic catheter for measuring intramuscular pressures. *J. Orthop. Res.* 8:464–468, 1990.
- <sup>7</sup>Davis, J., K. R. Kaufman, and R. L. Lieber. Correlation between active and passive isometric force and intramuscular pressure in the isolated rabbit tibialis anterior muscle. *J. Biomech.* 36:505–512, 2003.
- <sup>8</sup>Davis, J., K. R. Kaufman, and R. L. Lieber. Correlation between active and passive isometric force and intramuscular pressure in the isolated rabbit tibialis anterior muscle. *J. Biomech.* 36:505–512, 2003.
- <sup>9</sup>Degens, H., S. Salmons, and J. C. Jarvis. Intramuscular pressure, force and blood flow in rabbit tibialis anterior muscles during single and repetitive contractions. *Eur. J. Appl. Physiol. Occup. Physiol.* 78:13–19, 1998.
- <sup>10</sup>Go S. A., E. R. Jensen, S. M. O’Connor, L. Q. Evertz, D. A. Morrow, S. R. Ward, R. L. Lieber, and K. R. Kaufman. Design considerations of a fiber optic pressure sensor protective housing for intramuscular pressure measurements. *Ann. Biomed. Eng.* 1–8, 2016.
- <sup>11</sup>Harry, J. D., A. W. Ward, N. C. Heglund, D. L. Morgan, and T. A. McMahon. Cross-bridge cycling theories cannot explain high-speed lengthening behavior in frog muscle. *Biophys. J.* 57:201–208, 1990.
- <sup>12</sup>Hill, A. V. The heat of shortening and the dynamic constants of muscle. *Proc. R. Soc. Lond. B* 126:136–195, 1938.
- <sup>13</sup>Hug, F., K. Tucker, J. L. Gennisson, M. Tanter, and A. Nordez. Elastography for muscle biomechanics: toward the estimation of individual muscle force. *Exerc. Sport Sci. Rev.* 43:125–133, 2015.
- <sup>14</sup>Jenkyn, T. R., B. Koopman, P. Huijing, R. L. Lieber, and K. R. Kaufman. Finite element model of intramuscular pressure during isometric contraction of skeletal muscle. *Phys. Med. Biol.* 47:4043–4061, 2002.
- <sup>15</sup>Katz, B. The relation between force and speed in muscular contraction. *J. Physiol.* 96:45–64, 1939.
- <sup>16</sup>Kaufman, K. R., T. Wavering, D. Morrow, J. Davis, and R. L. Lieber. Performance characteristics of a pressure microsensor. *J. Biomech.* 36:283–287, 2003.
- <sup>17</sup>Kirkebo, A., and A. Wisnes. Regional tissue fluid pressure in rat calf muscle during sustained contraction or stretch. *Acta Physiol. Scand.* 114:551–556, 1982.
- <sup>18</sup>Koo, T. K., and M. Y. Li. A guideline of selecting and reporting intraclass correlation coefficients for reliability research. *J. Chiropr. Med.* 15:155–163, 2016.
- <sup>19</sup>Lieber, R. L., and F. T. Blevins. Skeletal muscle architecture of the rabbit hindlimb: functional implications of muscle design. *J. Morphol.* 199:93–101, 1989.
- <sup>20</sup>Nakhostine, M., J. R. Styf, S. van Leuven, A. R. Hargens, and D. H. Gershuni. Intramuscular pressure varies with depth. The tibialis anterior muscle studied in 12 volunteers. *Acta Orthop. Scand.* 64:377–381, 1993.
- <sup>21</sup>Ozderdem, U. Measuring interstitial fluid pressure with fiberoptic pressure transducers. *Microvasc. Res.* 77:226–229, 2009.
- <sup>22</sup>Rassier, D. E., and B. R. MacIntosh. Length-dependent twitch contractile characteristics of skeletal muscle. *Can. J. Physiol. Pharmacol.* 80:993–1000, 2002.
- <sup>23</sup>Sacks, R. D., and R. R. Roy. Architecture of the hind limb muscles of cats: functional significance. *J. Morphol.* 173:185–195, 1982.
- <sup>24</sup>Sejersted, O. M., and A. R. Hargens. Intramuscular pressures for monitoring different tasks and muscle conditions. *Adv. Exp. Med. Biol.* 384:339–350, 1995.
- <sup>25</sup>Styf, J. *Compartment Syndromes : Diagnosis, Treatment, and Complications*. Boca Raton: CRC Press, p. 301, 2004.
- <sup>26</sup>Styf, J., R. Ballard, M. Aratow, A. Crenshaw, D. Watenpugh, and A. R. Hargens. Intramuscular pressure and torque during isometric, concentric and eccentric muscular activity. *Scand. J. Med. Sci. Sports* 5:291–296, 1995.
- <sup>27</sup>Styf, J. R., A. Crenshaw, and A. R. Hargens. Intramuscular pressures during exercise Comparison of measurements with and without infusion. *Acta Orthop. Scand.* 60:593–596, 1989.
- <sup>28</sup>Ward, S. R., J. Davis, K. R. Kaufman, and R. L. Lieber. Relationship between muscle stress and intramuscular pressure during dynamic muscle contractions. *Muscle Nerve* 36:313–319, 2007.
- <sup>29</sup>Winters, T. M., G. S. Sepulveda, P. S. Cottler, K. R. Kaufman, R. L. Lieber, and S. R. Ward. Correlation between isometric force and intramuscular pressure in rabbit tibialis anterior muscle with an intact anterior compartment. *Muscle Nerve* 40:79–85, 2009.

**Publisher’s Note** Springer Nature remains neutral with regard to jurisdictional claims in published maps and institutional affiliations.